

Carbon Monitor Power - Simulators (CMP-SIM v1.0) across countries: a data-driven approach to simulate daily power **generation**

Léna Gurriaran^{1, 2}, Yannig Goude³, Katsumasa Tanaka^{1,4}, Binqing Zhu^{1,5}, Zhu Deng⁶, Xuanren Song⁵, Philippe Ciais¹

5 ¹Laboratoire des Sciences du Climat et de l'Environnement (LSCE), IPSL, CEA/CNRS/UVSQ, Université Paris-Saclay, Gif-sur-Yvette, France

²Atos, River Ouest, 95877 Bezons Cedex, France

³EDF Lab, 7 Boulevard Gaspard Monge, 91120 Palaiseau

⁴Earth System Division, National Institute for Environmental Studies (NIES), Tsukuba, Japan

10 ⁵Department of Earth System Science, Tsinghua University, Beijing, 100084, China

⁶Alibaba Cloud, Hangzhou, Zhejiang, 310030, China

Correspondence to: Léna Gurriaran (lena.gurriaran@lsce.ipsl.fr; lena.gurriaran@atos.net)

Abstract. The impact of climate change on power demand **and power generation** has become increasingly significant. **Changes** in temperature, relative humidity, and other climate variables **affect** cooling and heating

15 demand for households and industries **and, therefore, power generation**. Accurately predicting power **generation** is crucial for energy system planning and management. It is also crucial to understand the evolution of power

generation to estimate the amount of CO₂ emissions released into the atmosphere, allowing stakeholders to make informed plans to reduce emissions and **to** adapt to the impacts of climate change. Artificial intelligence techniques have been used to investigate energy demand-side responses to external factors at various scales in

20 recent years. However, few have explored the impact of climate and weather variability on power demand. This study proposes a data-driven approach to model daily power demand provided by the Carbon Monitor Power

project by combining climate variables and human activity indices as predictive features. Our investigation spans the years 2020 to 2022 and focuses on eight countries or groups of countries selected to represent different

25 climates and economies, accounting for over 70 % of global power consumption. These countries include

Australia, Brazil, China, the European Union (EU), India, Russia, South Africa, and the United States. We

assessed various machine-learning regressors to simulate daily power demand at the national scale. For countries

within the EU, we extended the analysis to one group of countries. We evaluated the models based on key

evaluating metrics: coefficient of determination (R²), Mean Absolute Error (MAE), Root Mean Squared Error

(RMSE), and Median Absolute Error (MedAE). We also used the models to identify the most influential

30 variables that impact power demand and apprehend their relationship with it. Our findings provide insight into variations in important predictive features among countries, along with the role played by distinct climate

variables and indicators of the level of economic activity, such as weekends and working days, vacations and holidays, and the influence of COVID-19.

1 Introduction

35 Climate significantly impacts power demand (Lucon et al., 2014; Isaac and van Vuuren, 2009), as the changes in temperature, relative humidity, and precipitation patterns affect the cooling and heating demand of households and industries (Mukherjee et al., 2019). Globally, climate change is expected to increase total power demand under low latitudes and decrease under temperate and high latitudes because of warmer winters (Van Ruijven et al., 2019). However, there remain large uncertainties in how climate change will affect power demand
40 (Deroubaix et al., 2021; Romitti and Sue Wing, 2022; Yalew et al., 2020) due to complexities associated with understanding the precise effects of different variables on power demand, whether they are climatic or socioeconomic. Improving comprehension of the complex interactions between these variables and power demand becomes crucial for accurately predicting and managing power **systems** across different timescales. Accurate predictions of power demand **and power generation** can help energy providers to optimize generation
45 and transmission, reduce costs, and improve the reliability of power supply at the seasonal scale. This becomes even more critical in the context of climate change, which has already begun to impact power demand and caused power outages in various parts of the world due to high cooling demand associated with exceptional heatwaves and other extreme climate events (Ahmad, 2021; Burillo et al., 2018). Finally, going one step further, understanding the impact of climate change on **the power sector** is essential for managing CO₂ emissions from the
50 power sector, as it is closely related to the development of strategies for reducing greenhouse gas emissions and adapting to changes in energy consumption patterns (Jiang et al., 2020).

Studies have started addressing the aforementioned question from both power generation and demand perspectives. Examining the weather sensitivity of the power sector from a generation perspective can provide valuable insights for addressing these issues. In particular, several studies showed that increasing renewable
55 generation capacity led to reduced baseload generation from fossil energy (Bloomfield et al., 2016, Silva et al., 2018), contributing positively to decarbonization. For example, increasing wind power generation in the UK reduced coal, gas, or nuclear power generation (Bloomfield et al., 2016). However, transition to renewables also increases the exposure of the power systems to climate variability (Craig et al., 2018, Elliston et al., 2013, Silva et al., 2018).

60 Other studies present approaches to identify meteorological, socioeconomic, and technical drivers for power demand and sectoral power production (Bloomfield et al., 2020, Toktarova et al., 2019). Such approaches provide improved means to quantify the impacts of climate change on the power system and are adaptable to different geographical locations. In addition, some studies focus on the development of databases that can be used for investigating the climate sensitivity of the power sector and the impacts of climate change, such as the C3S
65 Energy database developed by Dubus et al. (2021), which provides power demand and power supply data for Europe.

Electricity demand modeling often uses multi-linear models to integrate various influencing factors (Bloomfield et al., 2016 and 2020, Delort Ylla et al., 2023, Tantet et al., 2019, Toktarova et al., 2019). While such multi-linear models may appear more intuitive and simpler than machine learning models, they do not necessarily imply
70 easier implementation and may require significant manual parameter tuning. Furthermore, machine learning models and semiparametric additive approaches, such as General Additive Models (GAM), are already widely used in the load forecasting community (Dordonnat et al., 2016, Fan and Hyndman, 2012, Nedellec et al., 2014, Obst et al., 2021, Pierrot and Goude, 2011) and have demonstrated superior forecasting capabilities compared to multilinear models (Hong et al., 2016).

75 While artificial intelligence techniques use has grown to investigate energy demand-side responses at various spatial and temporal scales (Antonopoulos et al., 2020), literature on the impact of climate and weather variability on power demand using these methods is still limited. Previous studies have primarily been developed for specific regions or countries (Mohammadiziazi and Bilec, 2020; Hiruta et al., 2022a; Hiruta et al., 2022b; Gurriaran et al., 2022a; Gurriaran et al., 2022b). Until recently, there was no comprehensive worldwide dataset
80 for daily power dynamics across multiple countries. This knowledge gap has been filled with the introduction of the Carbon Monitor Power data (Zhu et al., 2023), which provides daily estimates of power demand at the national level for about forty countries, along with detailed sources of supply. In this study, we use this newly available dataset to develop a machine-learning approach for modeling daily power demand by combining climate variables and human activity indices, considering the impact of climate through cooling and heating
85 demand proxies. In addition, we consider human activity indices, such as working days, weekends, and holidays, as well as the level of stringency of COVID-19 measures, which play a crucial role in determining power demand as they reflect the level of economic activity (Antoniadis et al., 2022; Hiruta et al., 2022b).

Building on our earlier work on Qatar and Japan (Gurriaran et al. 2022a, 2022b), the present study aims to develop data-driven models that simulate daily power demand for a large number of countries with contrasted
90 climates based on the Carbon Monitor Power demand dataset, and a comprehensive set of daily climate variables

and human activity indices. Additionally, the study aims to infer the most important variables for each country or region and discuss differences that may arise between the countries. The data we used include total daily power production at a national or regional scale from 15 February 2019 to 15 October 2022, climate variables, and human activity indices to develop models at a national or regional scale. Our study assumes that daily power
95 production is equal to power demand, as transmission losses are assumed to be negligible. The dataset is divided into a learning set and a test set. Different machine-learning regressors are trained on the learning set to develop the models for power demand prediction. The performance of the models is assessed using the test set through error metrics, the evaluation of overfitting, and an analysis of the model's residuals.

Our models have a multifaceted goal that includes separating climate factors that drive power demand variations,
100

conducting cross-country comparative analysis of these factors, understanding the relationship between power and climate extremes, and developing predictive models for various applications. Our research aims to comprehensively understand the intricate interplay between climate and power demand by isolating specific climatic elements that influence energy consumption and comparing global variations. The main goal is to provide predictive models that can be used for different timeframes. This will help improve decision-making in
105 energy management for short-term grid optimization, seasonal resource planning, and long-term strategies that align with changing climate scenarios. These models could be applied in various contexts. They could be used to define new responsive power production modules coupled with weather forecast models to enable operational production forecasting. They could also benefit the domain of air quality monitoring; for example, the models could be integrated into data assimilation systems of atmospheric composition, such as the global Copernicus
110 Atmosphere Monitoring Service (CAMS) and regional models, which require interactive emissions fields with weather and human activity variations. Furthermore, our models may be used for adapting power systems to climate extremes. Finally, they may be incorporated into longer-term climate scenarios assuming that the short-term climate response of power production will remain unchanged. Some of our models can even integrate hypotheses relative to changes in consumption habits.

115 We present models for eight countries or groups of countries. Those countries represent diverse climates, economies, and populations worldwide: Australia, Brazil, China, the European Union (including the United Kingdom, referred to as EU27 & UK), India, Russia, South Africa, and the United States. Those countries are all significant in terms of population, GDP, power production, and CO₂ emissions. Together they represent about 50

120 % of the world's total population, 67 % of the global GDP, and 80 % of total power generation in 2021 (IEA, 2021). For the sake of presentation, we present the results for EU27 & UK in the main text as an illustration. The results for other countries are provided in the Supplementary Materials (Sect. 2).

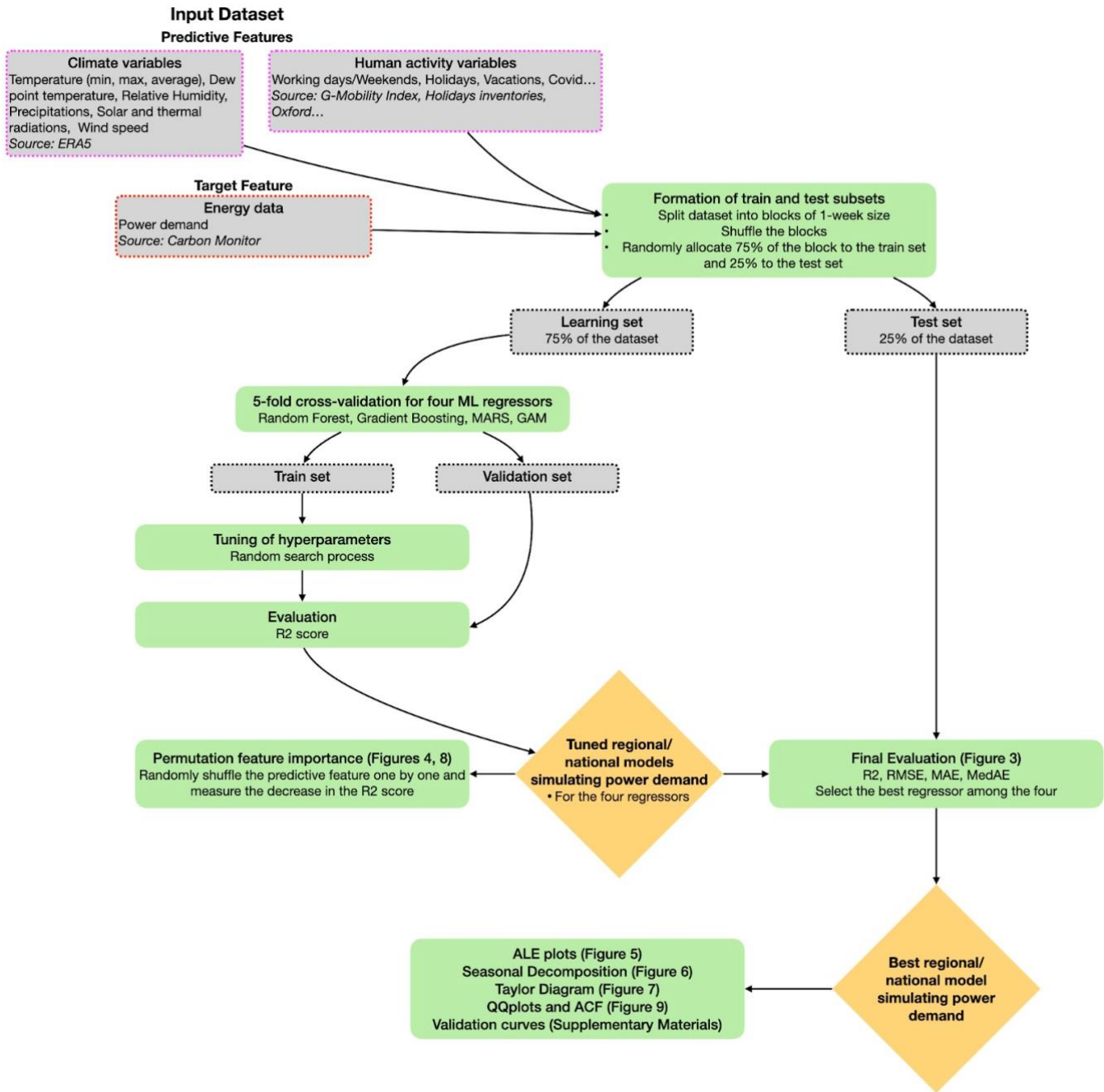


Figure 1. Methodological flowchart of this study: CMP-SIM approach.

2 Data

125 This section describes the input data used to develop the regional or national models simulating power demand: the Carbon Monitor Power – Simulators (CMP-SIM v1.0). Regional power demand refers here to the power demand of EU27 & UK. All the data are at a national or regional level and at a daily timescale. The data were pre-processed to a format suitable for the machine learning approach. We used 32 months of input data from 15 February 2020 to 15 October 2022.

Predictive Features					
	Variable Name	Unit	Description	Country/Region	Source
Climate Variable	T2M	°C	Average daily surface air temperature at 2m	All	ERA5
	T2Mmax	°C	Maximum daily surface air temperature at 2m		
	T2Mmin	°C	Minimum daily surface air temperature at 2m		
	Td	°C	Average daily dew point temperature at 2m		
	RH	%	Average daily relative humidity		
	Surface Pressure	Pa	Average daily pressure of the atmosphere on the surface of the land		
	U	m.s ⁻¹	Average wind speed and direction at 10m		
	TP	m	Average daily total precipitation		
	SSRD	J.m ⁻²	Surface solar radiation downward		
Human Activities Indices	STRD	J.m ⁻²	Surface thermal radiation downward	All	Python repository
	DOW	-	Day of week – categorical variable from 0 to 6		
	Holidays	-	Categorical variable 0 or 1		Manually collected
	Workplace	%	Changes of workplace occupancy compared to a baseline		Google Community
Covid				All	Mobility Reports Mathieu et al., 2020
	Covid	-	COVID-19 stringency index		

TOY	-	Numerical day of year	China and EU	-
GDP	%	Quarterly GDP growth rate	Only China	China Bureau of Statistic
Target Feature				
Variable Name	Unit	Description	Country/Region	Source
Power Data	Total Demand	GWh	Total daily power demand in the region considered	All Carbon Monitor - Power

130 **Table 1. Input and output dataset for this study**

2.1 Predictive features

The predictive features used to build models predicting power demand, including climate variables and human activity indices (Table 1), are described in the following.

135 Climate Variables: The climate variables include temperature (daily average, max, and min), dew point temperature, surface pressure, relative humidity, wind, precipitation, and solar radiation. These variables are known to impact power demand, as they affect the energy consumption patterns of households and industries. The climate variables are obtained from the ERA5 reanalysis at a daily timescale (Muñoz Sabater, 2019). All the climate variables were weighted by population density (CIESIN) to give more importance to climate over densely populated areas, as these regions are accountable for a significant proportion of power demand.

140 Human Activity Indices: Human activity data (Fig. 2), such as working days, holidays, and school vacations, also play a crucial role in determining power demand, as they reflect the level of activity influencing the power demand. These indices are obtained from publicly available datasets.

145 The effect of working days and weekends on power demand is accounted for with the numerical variable DOW (Day Of Week), where the value zero corresponds to Monday, one to Tuesday, and so forth, with six representing Sunday. To account for the effect of holidays, we introduce the variable “Holiday”, which takes the value of one if the day is a holiday and zero otherwise.

Because our data cover the COVID-19 period, we accounted for the impacts of COVID-19-related measures on power demand using the COVID stringency index. We used the COVID stringency index, which aggregates information from various policy sources, including the Oxford COVID-19 Government Response Tracker (Hale 150 et al., 2021) and the ACAPS COVID-19 Government Measures Dataset (ACAPS COVID-19). The COVID

stringency index is a composite measure comprising nine response indicators, such as school closures, workplace closures, and travel bans. The values of these indicators are rescaled on a scale of 0 to 100, where 100 represents the strictest level of response. The COVID stringency index is available for 207 countries (Mathieu et al., 2020).

155 Additionally, we used data from the Google Community Mobility Reports to account for the effect of vacations on power demand. Google developed these reports to track the effects of COVID-19 on the frequency of various types of locations and was available from 15 February 2020 to 15 October 2022 (Google LLC., 2020). These reports are constructed by analyzing location data from users who have opted into Location History for their Google account, and the data are aggregated to preserve users' anonymity. The reports indicate how visits and length of stay in these different location categories have changed over time compared to a baseline period before 160 the COVID-19 pandemic from 3 January 2020 to 6 February 2020. Specifically, we used the "workplaces" metric, which reflects the change in the percentage of people present at their workplaces compared to the baseline reference period. To remove the effects of weekends and holidays in the workplace metric, we applied a running mean on a 7-day basis and replaced the values of the holiday days to match the value of the previous day. This was done because the effects of weekends and holidays are already represented by the variables "DOW" and 165 "holidays," respectively. However, the Google Community Mobility Reports data are unavailable for China and the EU (Table 1). Thus, we employed an alternative variable, namely "Time of the Year" (TOY), to reflect the level of economic activity in the two countries. This variable is defined as the numerical day of the year, ranging from one on January 1st to 365 or 366 on December 31st. TOY is an alternative to Google Mobility data because it can serve as a proxy for economic activity by allowing the possible seasonal variation of power demand 170 throughout the year to be linked to a specific period within that year.

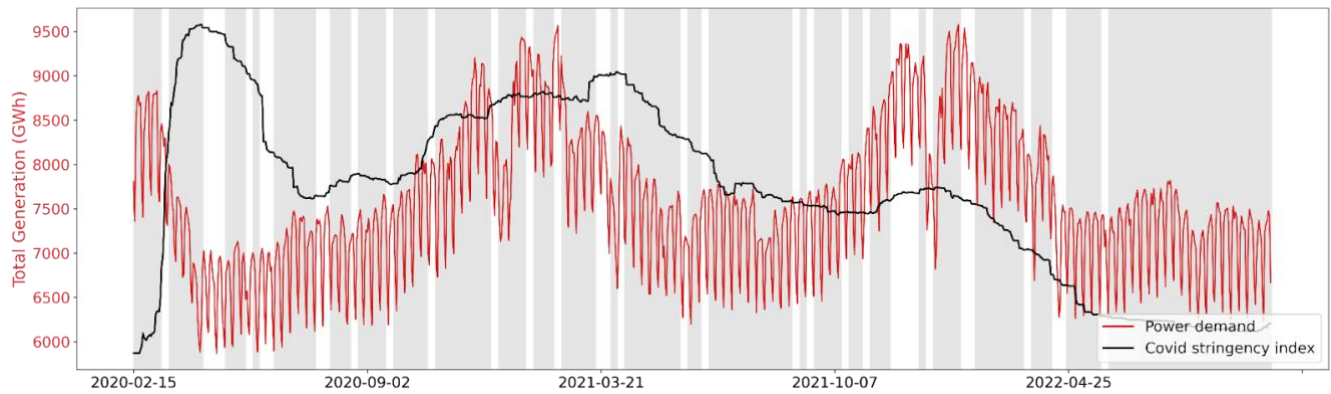
Finally, given the significant reliance of China's power demand on its industrial sector, it is imperative to consider economic indicators that reflect changes in industrial activity. We hypothesized a strong relationship between GDP and industrial activity and assumed that the fluctuations in GDP could be used as a proxy for changes in industrial activity. Consequently, we added quarterly GDP as a predictive feature for China.

175 In total, 15 predictive features were used to simulate daily power demand. However, the exact number and combination of predictive features used to simulate power demand vary depending on the availability of human activity data for a particular country and the use of GDP.

2.2 Target features

The target feature of this study, i.e., the data we aim to simulate, are the total daily power demand at the regional 180 or national scale (Fig. 2). This feature is calculated from the publicly available Carbon Monitor - Power dataset

(Zhu et al., 2023; Liu et al., 2020a; Liu et al., 2020b). This dataset includes daily historical data on electricity generation from 37 countries since January 2019. It gives the electricity generated by different energy sources: fossil (coal, gas, and oil), renewable (solar, wind, hydro, and others including biomass, geothermal, etc.), and nuclear. We obtain the total daily power demand by summing the daily power generation of each source under 185 the assumption that demand is equal to generation. One outlier was detected for India (19 April 2020) and removed from the dataset.



190 **Figure 2. Evolution of human activity predictive feature from COVID stringency index for EU27 & UK and power demand over the studied period. The shaded area represents the learning periods, and the blank area the test periods.**

3 Model Development

This section describes the approach we developed for establishing national or regional models simulating daily power demand from the predictive features described in Sect. 2.1 (Fig. 1). The models have been coded in Python 195 version 3.6.12. Our approach follows machine-learning procedures (Raschka, 2018; Raschka and Mirjalili, 2019), including the formation of learning and test subsets, random search with cross-validation, regressor training on the learning set and performance evaluation with error metrics on the test set, model interpretation with model 200 agnostic interpretability methods (ALE plots and permutation feature importance), and validation curve analysis to detect potential overfitting or underfitting. Previous studies have applied similar approaches to various countries. For example, in Japan, Hiruta et al. (2022a) used a machine-learning approach to derive temperature response functions at an hourly timescale. In previous works, we have developed data-driven models for long-term predictions in specific regions, namely Qatar (Gurriaran et al., 2022a) and Japan (Gurriaran et al., 2022b). The approach developed for Japan was more detailed and tailored to the country. It included a separate model for

carbon intensity and was conducted on the Japanese regional scale. The approach presented in this study is more

205 generic and can be applied to any country or region worldwide so long as daily data are available.

3.1 Partitioning of input data into learning and test subsets

We followed a consistent procedure for each country or region, as illustrated in Fig. 1. The first step is to divide the input dataset into learning and test subsets. This is a necessary step to examine the robustness of the results; machine-learning regressors will be trained on the learning set, and the performances of the models will be 210 evaluated on the test set. The entire dataset is divided into blocks of one-week size. Then, all these blocks are shuffled randomly. Once the shuffling is done, 25 % of the data are assigned to the testing subset and 75 % to the learning subset (Fig. 2). This ratio is common for partitioning the dataset into learning and test subsets (Raschka, 2020; Raschka and Mirjalili, 2022). This process ensures that both subsets are representative of the whole dataset and that the results obtained are robust and reliable.

215 3.2. Random search with cross-validation and evaluating metrics

We evaluate four machine-learning regressors: Random Forest (RF) (Breiman, 2001), Gradient Boosting (GB) (Fisher, 1958; Chen and Guestrin, 2016; Ke et al., 2017), Multivariate Adaptive Regressions Splines (MARS) (Friedman, 1991), and Generalized Additive Model (GAM) (Hastie and Tibshirani, 1990). RF and GB are two ensemble learning methods. RF combines multiple decision trees to make more accurate predictions. Each 220 decision tree is trained on a random subset of the training data to reduce the risk of overfitting. When making a prediction, RF takes the average prediction of all the decision trees in the ensemble. GB combines weak learners to form a stronger predictor. Each weak learner is trained sequentially to minimize the errors of the previous weak learners. This process is repeated until the error is minimized or a specified number of weak learners is reached. The final prediction is made by combining the predictions of all the weak learners. MARS and GAM are 225 two interpreted machine-learning methods for regression analysis. MARS uses a sum of piecewise linear regressions to model non-linear relationships, while GAM uses a sum of smooth functions such as splines. For GAM, we specified an equation for each country using the backward feature selection process (Wood, 2017). The model was executed using all the predictive features; then, we gradually eliminated all non-significant features until the model's stability was achieved according to a Fisher test. The allocation of a specific number of splines 230 to each feature was accomplished using an integer value approximately $\frac{1}{3}$ higher than the degree of freedom estimated by the GAM regressor during the initial run.

All regressors are trained on the learning set, and their hyperparameters are optimized through a random-search process with 5-fold cross-validation on the same subset. The cross-validation process involves partitioning the learning data into multiple subsets (here 5) and uses each subset in turn as a validation set to assess the model's 235 performance. The final evaluation of the model is done on the test set. The hyperparameters are the settings of the regressors that need to be specified before the training phase. They are specific to the type of regressor used and cannot be learned from the data. Optimizing the values of the hyperparameters is important as they can impact the accuracy and performance of the models. Grid search and random search are two common techniques to tune 240 hyperparameters. Grid search exhaustively searches through all possible combinations of hyperparameters, while random search randomly samples hyperparameters from a specified distribution. In a random search, the number of combinations tried is controlled by a pre-determined number of iterations (`n_iter`). The high computational cost of grid search led us to choose random search to explore the hyperparameter space for RF, GB, and MARS. Limiting the number of iterations to 200 considerably reduced the computation time while giving satisfying 245 results. For GAM, we optimize only two hyperparameters. The description of the hyperparameters optimized through the random search process can be found in the supplementary materials (Sect. 1).

We calculated various error metrics to evaluate the performance of the models on the test set. These include the coefficient of determination (R^2), Mean Absolute Error (MAE), Root Mean Squared Error (RMSE), and Median Absolute Error (MedAE). The objective is to maximize R^2 and minimize the values of MAE, RMSE, and MedAE.

250 **3.3. Interpretation of the models with permutation feature importance and ALE plots**

Permutation feature importance and ALE plots are two methods that allow the interpretation of non-directly 255 interpreted machine learning models such as RF and GB regressors. We use the permutation feature importance to classify the predictive feature by order of importance and the ALE plot to understand the relationship between the predictive features and the target feature. For consistency in our results, we also apply this method to GAM and MARS regressors even though they are interpreted machine learning models.

Permutation feature importance enables a relative classification of features within the models, identifying the 260 most significant predictive features to explain power demand for a particular country. We calculate a permutation score for each predictive feature with the four machine-learning regressors tested. This score is determined by randomly shuffling the feature and measuring the reduction in model accuracy that results. The feature is shuffled five times; then, an average score is calculated.

ALE plots enable interpreting the relationship between the target feature (power demand) and one particular predictive feature (Apley and Zhu, 2020). They represent the influence of the predictive feature on the target feature when the other predictive features are held constant. ALE plots are used to identify the non-linearities between the target feature and predictive features. In this study, ALE plots were calculated for all predictive features included in the model that achieved the best evaluation metrics. This calculation involves dividing the range of the feature into intervals, calculating the average power demand for each interval, determining the differences in prediction between adjacent intervals, and integrating to estimate the individual influence of a feature.

3.4. Model validation: validation curves, quantile-quantile diagrams, autocorrelation, and seasonal decomposition

Validation curves are commonly used to detect overfitting or underfitting problems. Overfitting happens when a model is too complex and fitted to the training data to the point that the model cannot be generalized to other data. In this case, the model performs well on the train sets but poorly on the validation set. Two validation curves are calculated, one for the train set and one for the validation set to detect overfitting. Those curves show how the model's performance (here measured with R^2) changes for both subsets as a particular hyperparameter value of the model is varied. If the model performs much better on the train set than on the test set or the two curves diverge above a certain hyperparameter value, it indicates overfitting issues. In this study, we also used the validation curves to verify that the correct hyperparameter values were selected during the random search process. Underfitting is detected when the performances of the model are poor on both subsets. The validation curves for all countries considered can be found in Supplementary Materials (Sect. S2).

Assumptions underpinning statistical methodologies are critical for ensuring the validity of analyses. One of our methodological assumptions is the normality of the residuals obtained from power demand calculations using our statistical models. To verify this assumption, we constructed quantile-quantile (QQ) plots for the residuals obtained from the four regressors (Chambers, 1983). These plots display the quantiles of a dataset as a function of the corresponding theoretical quantiles of a normal distribution. If the points on the QQ plot align closely with the diagonal, it indicates that the residuals follow a normal distribution, supporting the suitability of our methodology for accurately simulating power demand from the given data.

Assessing the temporal structure of the residuals of a model is another way to evaluate the validity of a time-series model. Autocorrelation plots represent the correlation between a time-series and its delayed version. We constructed autocorrelation plots for the residuals of our four power demand regression models to identify any

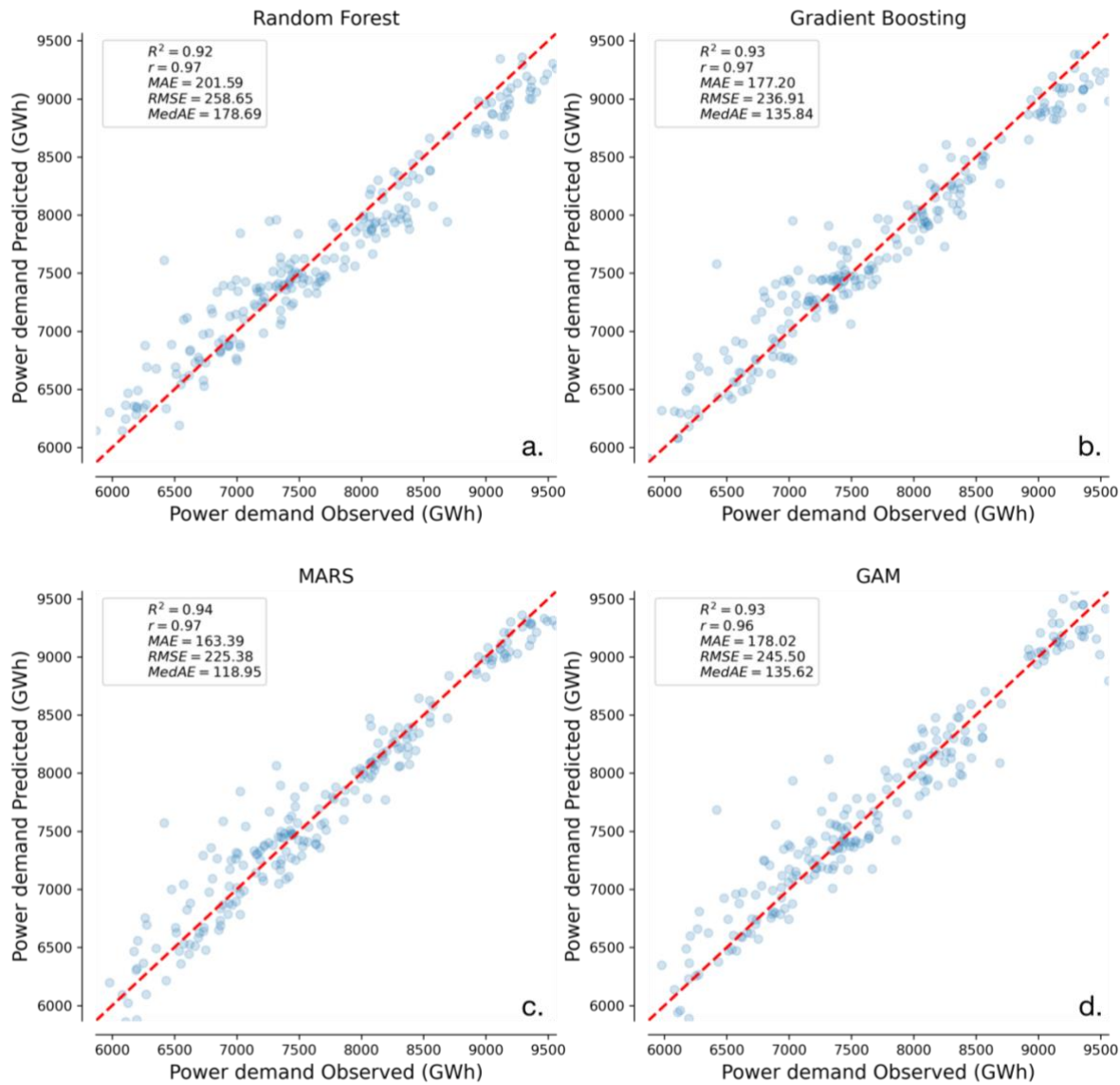
remaining temporal structures that the models may not have captured. To ensure the inclusion of weekly information, we chose a maximum time lag of 14 days for our analysis. If the autocorrelation values decrease rapidly as the lag increases, it suggests that our models have fully explained the temporal information. Conversely, if the autocorrelation values remain high at larger lags, some relevant temporal information may not 295 have been captured.

Finally, we used time-series seasonal decomposition to assess the performances of our models at different time scales. Seasonal decomposition is a statistical technique that decomposes a time-series into different components: trend, seasonality, and residuals (Hyndman and Athanasopoulos, 2018). The trend component represents the long-term trend of the data, and the seasonality component captures the periodicity in the data (i.e., weekly, 300 seasonal, or annual cycles). The residuals component is the random variations in the data that cannot be explained by the seasonal decomposition method. For this study, we used a simple decomposition method based on moving average with an additive model: $PD_t = T_t + S_t + R_t$, where PD_t is the power demand time-series, T_t is the “trend” component, S_t is the “seasonality” (here weekly) component, and R_t is the residual component. T_t is estimated using a convolutional filter and then subtracted from PD_t . S_t is obtained by averaging the de-trended 305 series for each period. In this study, we did this analysis with a seven-day period to capture the weekly seasonality. This seasonal decomposition method was applied to the four time-series obtained with our models and to the original power demand time-series to serve as a point of comparison.

4 Results: Output of the models

This section presents the main outputs of our machine-learning approach with a focus on EU27 & UK: the 310 performance of the different models tested, the permutation feature importance, and the ALE plots. The results for other countries can be found in the Supplementary Materials (Sect. 2).

Scatter plots show the modeled vs. observed power demand, with corresponding error metrics displayed on each subplot (Fig. 3). In the case of the EU27 & UK, all regressors perform similarly in evaluating metrics. R^2 Table 2 provides a summary of the evaluation metrics for all countries.



315

Figure 3. Comparison of machine-learning regressors performance for EU27 & UK. Predicted power demand plotted against observed power demand for the four machine-learning regressors tested: (a) RF, (b) GB, (c) MARS, and (d) GAM. The red dashed line represents the 1:1 line of perfect agreement between predictions and observations.

320

Comparing the results of all countries, the models perform best in predicting power demand for Russia, with an R^2 of 0.98. In contrast, they exhibit the poorest performance for China, with an R^2 always under 0.8 (Table 2).

The results presented in Table 2 do not reveal a single best regressor that consistently outperforms others across all countries.

325

		Australia	Brazil	China	EU27 & UK	India	Russia	South Africa	United States
	R ²	0.80	0.87	0.75	0.92	0.85	0.96	0.81	0.89
Random Forest	MAE	12.7	41.5	893.4	201.6	106.9	53.5	13.7	306.2
	RMSE	16.7	59.8	1161.9	258.7	149.1	72.0	18.7	394.1
	MedAE	10.2	29.1	732.1	178.7	76.3	38.6	10.8	250.5
	R ²	0.84	0.93	0.77	0.93	0.83	0.98	0.77	0.91
Gradient Boosting	MAE	10.9	33.6	872.5	177.2	112.2	44.6	15.0	280.1
	RMSE	14.6	42.4	1128.6	236.9	159.3	58.7	20.6	361.4
	MedAE	8.4	28.4	666.3	135.8	78.5	35.5	11.7	216.9
	R ²	0.83	0.92	0.78	0.94	0.80	0.97	0.83	0.90
MARS	MAE	11.5	36.2	810.3	163.4	121.8	50.3	13.02	309.2
	RMSE	15.1	46.5	1106.6	225.4	173.2	66.8	17.8	388.0
	MedAE	10.3	28.4	635.9	118.9	80.1	42.3	10.4	248.3
	R ²	0.81	0.92	0.77	0.93	0.81	0.97	0.83	0.94
GAM	MAE	11.7	37.1	889.8	178.0	127.5	46.9	13.7	22.1
	RMSE	16.2	45.6	1120.1	245.5	171.6	64.1	17.9	292.7
	MedAE	9.0	33.1	753.9	135.6	105.6	34.9	11.4	169.3

Table 2. Comparison of the performances of the four machine-learning regressors for the countries studied with the four metrics: R², MAE, RMSE, and MedAE.

Figure 4 shows the five most important predictive features, as determined by the permutation feature importance.

330 When focusing only on predictive climate features (pink in Fig. 4), all regressors recognize temperature as a significant predictor, featuring it within the top five variables. However, the specific temperature-related feature that emerges as significant differs among the models (T2M, T2Mmax, T2Mmin, or Td). Furthermore, the variable SSRD (solar radiation) consistently appears as a crucial predictor, as it is included within the top five predictors for all regressors except MARS. These results underscore the crucial role of climate-related features in 335 predicting power demand. On the other hand, the analysis also highlights the relevance of human activity

features, with DOW, Covid, and TOY (blue in Fig. 4) always among the top five predictors. It is noteworthy that the order of the top five predictors varies across different models.

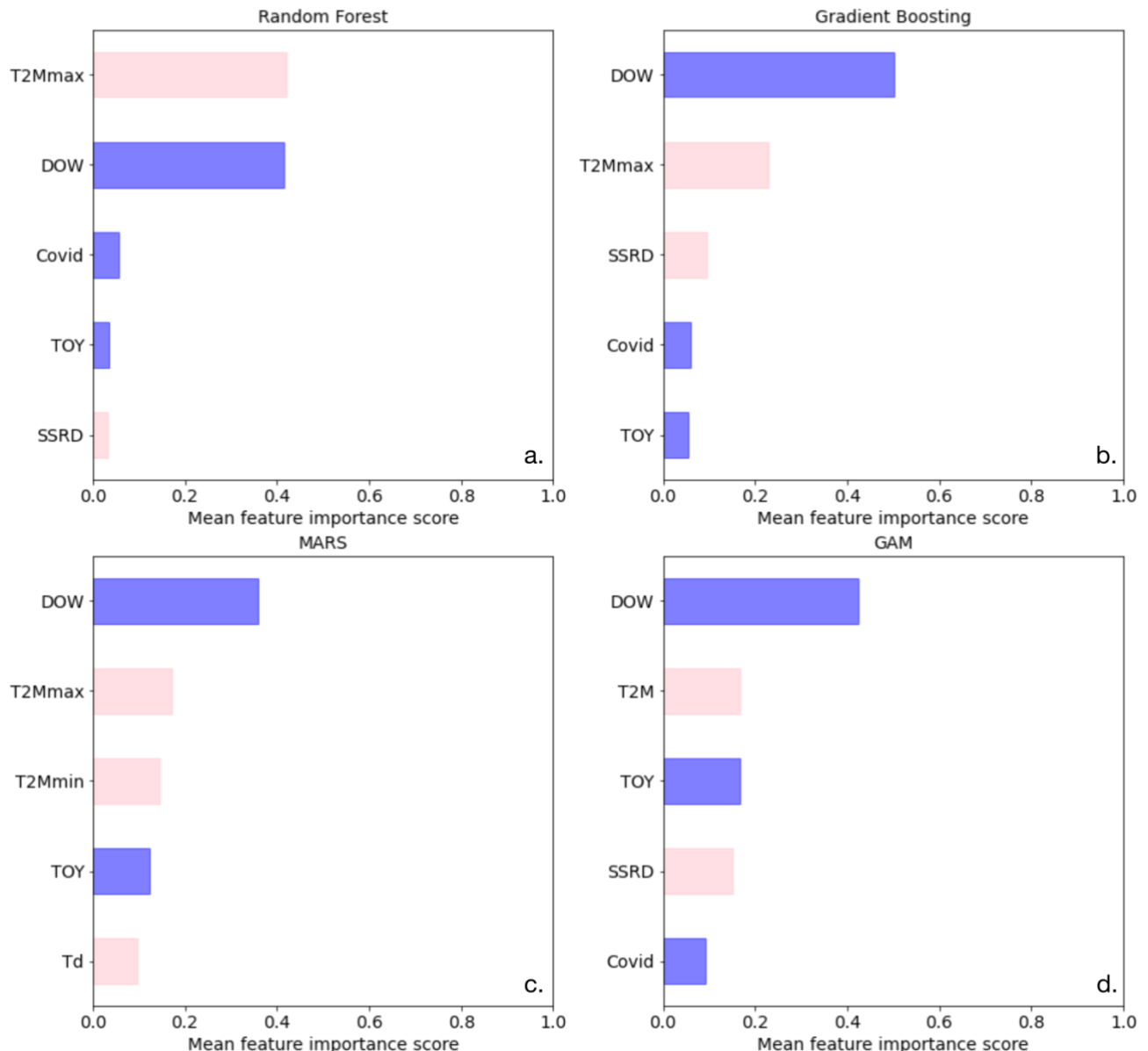
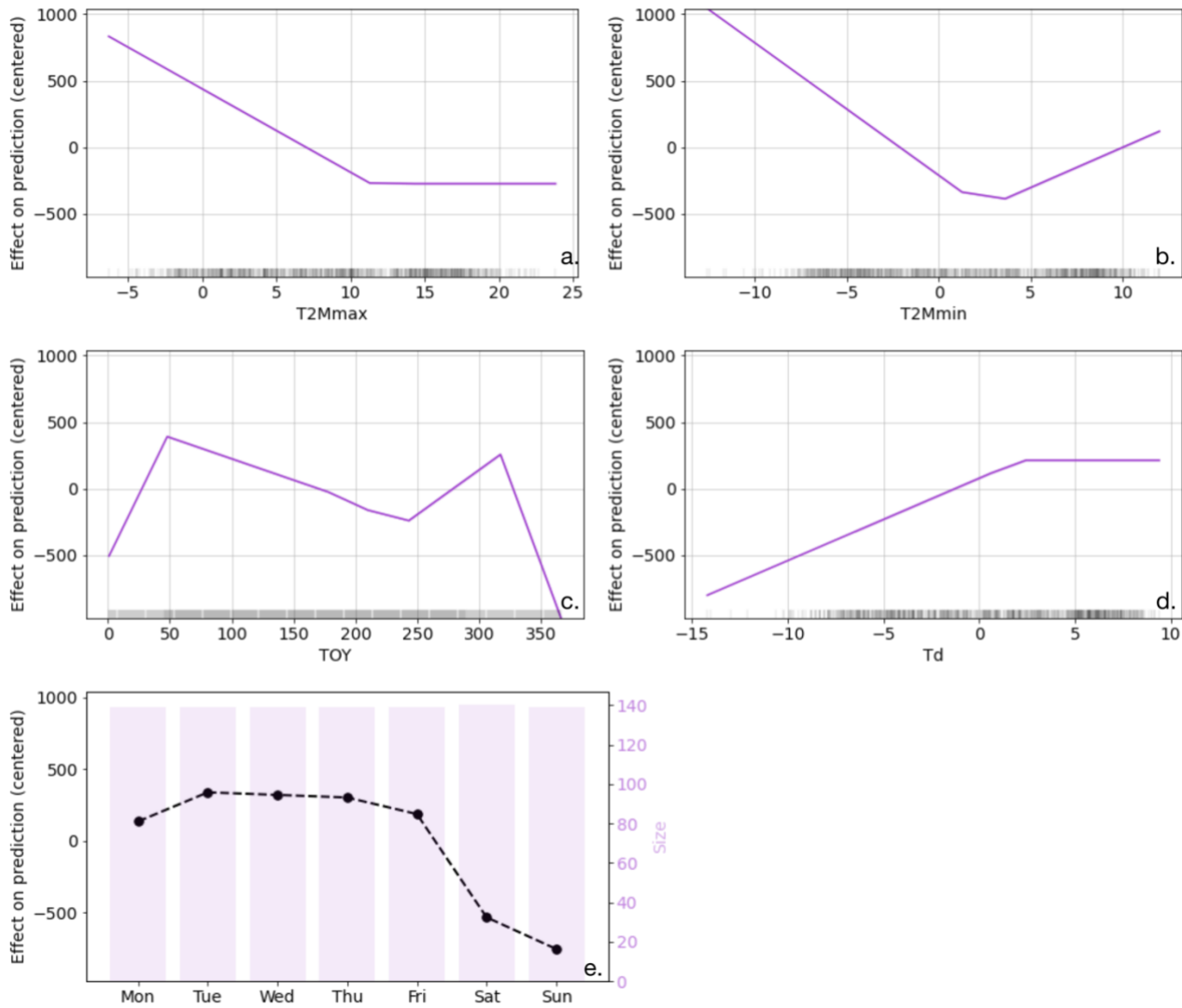


Figure 4. Permutation feature importances of the five most important predictive features from four different machine-learning regressors for EU27 & UK: (a) RF, (b) GB, (c) MARS, and (d) GAM.

ALE plots were generated for the top five predictive features with the MARS regressor, which performed best for EU27 & UK (Fig. 5). The ALE plots confirm the strong impact of temperature-related predictors on power demand, with Td, T2Mmax, and T2Mmin being particularly influential. ALE plots for Td demonstrate a positive correlation between power demand and heating (when the temperature is decreasing), and ALE plots for T2Mmax have a positive correlation for cooling (when the temperature is increasing) requirements. ALE plot for T2Mmin shows both effects. Examining the ALE plot for DOW (day of the week) reveals that power demand holds less significance during weekends than on weekdays. Finally, the ALE plot for TOY shows a decrease in power demand at the end and beginning of the year, corresponding to the holiday season. Overall, our findings here illustrated for EU27 & UK suggest that both climate and human activity factors are crucial in predicting power demand, and a comprehensive approach that considers both these aspects is needed to yield more accurate results.

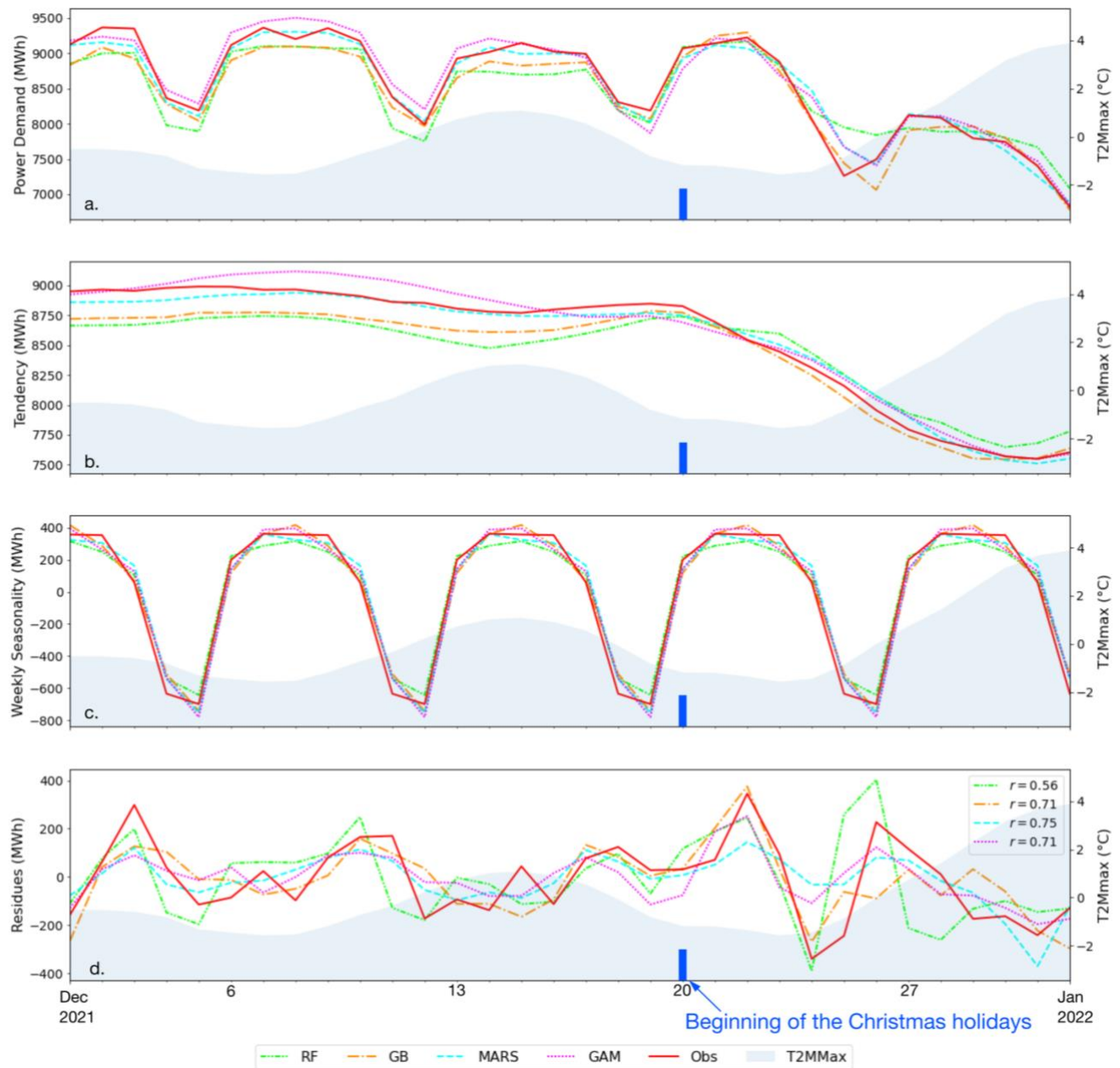
345

350



355

Figure 5. ALE plots of the effect of the top-five predictive features from MARS for EU27 & UK: (a) T2Mmax, (b) T2Mmin, (c) TOY, (d) Td, and (e) DOW, where size represents the number of days in each category. Each ALE plot shows the partial dependence of the target feature on a predictive feature while keeping all other features constant. The x-axis represents the values for each feature, and the y-axis represents the corresponding change in the predicted value of the target feature.



360 **Figure 6. Weekly seasonal decomposition analysis of the daily power demand data from four different**
models (RF, GB, MARS, GAM) as well as the observed data (Obs) for EU27 & UK: (a) Observed and
modeled daily times series, (b) trend component, (c) weekly component, and (d) residual component. The
legend in panel d represents the Pearson correlation coefficient between the models' residues and the
observations' residues. The shaded area in the plots represents the maximum daily temperature
365 **(T2Mmax) in a 7-day running mean.**

The comparison of the modeled decomposed times series and the observed decomposed time-series enable assessment of the ability of models to capture the diverse temporal patterns inherent in the data. By decomposing the time-series generated by the models and comparing them with observed electricity demand, it becomes possible to evaluate the models' ability to accurately replicate the various temporal patterns evident in the 370 observational data. Figure 6 focuses on December 2021 to illustrate the negative impact of the Christmas holidays on power demand. Electricity demand remains low at the end of the month, possibly due to the high temperatures observed during this period. The trend component (Fig. 6b) indicates that all models successfully capture the decrease in power demand attributed to the Christmas break. Upon comparing the seasonal decomposition of the models with that of the observational data, it demonstrates that GB exhibits the highest 375 accuracy in simulating this decrease in power demand. Additionally, our analysis demonstrates that all models perform well in simulating the weekly component (Fig. 6c). Lastly, our investigation reveals a correlation between the residuals of the seasonal decomposition of the models and those of the observations. This finding suggests that the models effectively capture short-term temporal patterns in electricity demand, indicating their potential to be used for generalization.

5.1 Model inter-comparison in different countries

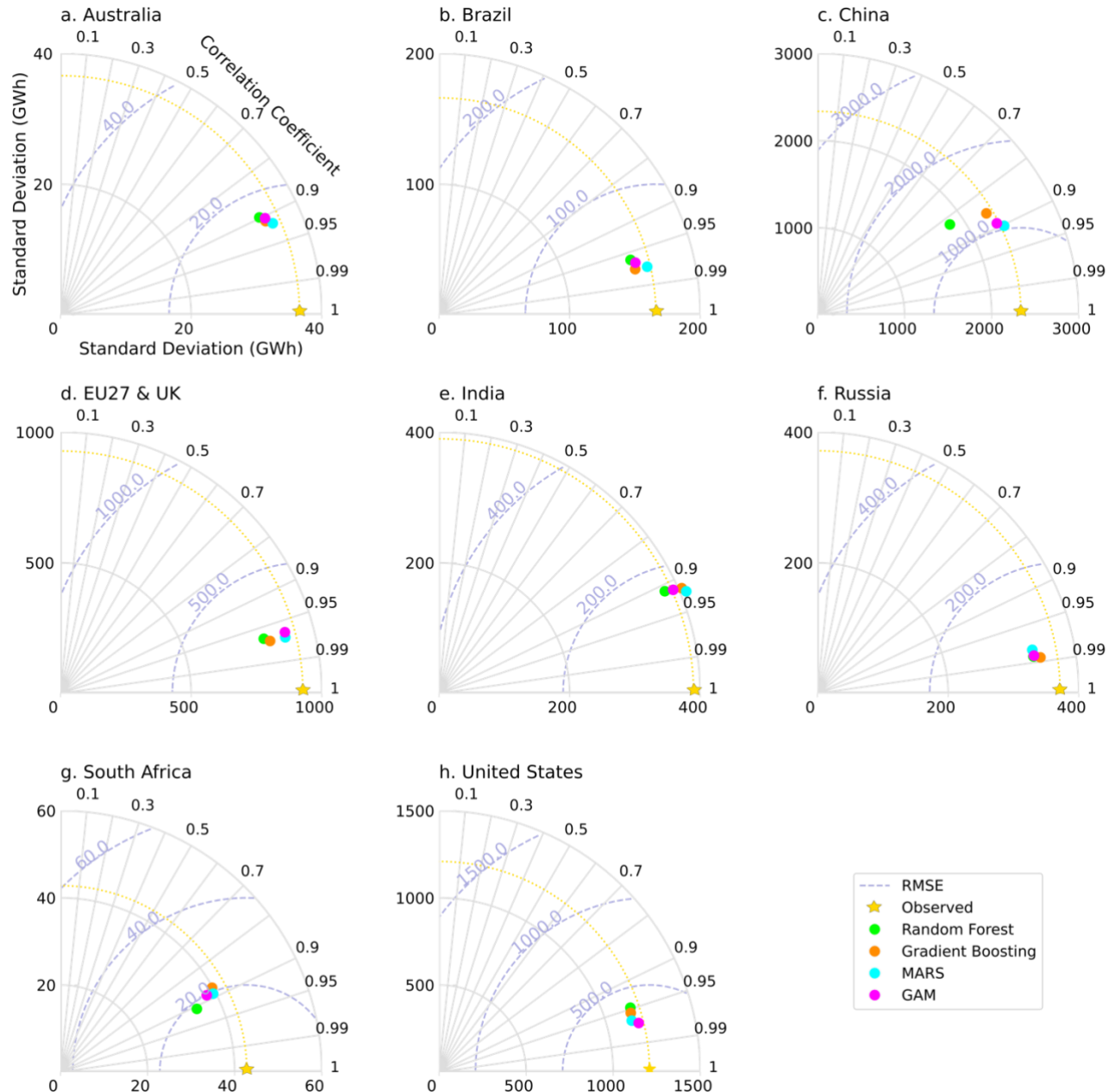


Figure 7. Taylor diagram for simulated power demand for the eight countries or regions. The colors indicate the different regressors tested: green, RF; orange, GB; blue, MARS; purple, GAM. The radial

385 **axis indicates the standard deviation, the angular axis the coefficient of correlation (R), and the dashed circles the RMSE.**

390 To compare the performance of our models against the (test) observation and across the eight countries or regions, we constructed Taylor diagrams for each country (Fig. 7). These diagrams provide a comprehensive visualization of how well the models compare to the reference data for each country in terms of correlation, RMSE, and standard deviation (Taylor, 2001). The results from the Taylor diagrams confirm what was observed in the previous section with the evaluating metrics (Table 2). Specifically, the performance of each model is similar for a given country or region, while it differs across countries. The models exhibit the best correlation 395 with observation for Russia (close to 0.99), closely followed by the United States, EU27 & UK, and Brazil, with a correlation higher or very close to 0.95. For Australia, China, India, and South Africa, the correlation is around 0.90. Except for India, the models underestimate the standard deviation of daily power demand.

400 One of the objectives of our study is to identify the most influential features on power demand for each country or region and to investigate whether any similarities exist across the different countries. A comparison of feature importance for each country and model (Fig. 8) is conducted to achieve this objective. Our results suggest that temperature-related features, including T2M, T2Mmax, T2Mmin, and Td, are always the primary climate drivers of power demand in all examined countries, indicating their significant influence on power demand across different regions. The other climate-related features included in this study do not appear to significantly drive power demand, except for SSRD, which slightly influences power demand for some countries in the RF, GB, and 405 GAM models.

410 Regarding human activity predictors, we observed significant variations in their importance across different countries and machine-learning regressors. For instance, the DOW feature shows high importance in some countries while insignificant in others, similarly for workplaces activity from Google Mobility data. In general, the different models found the same features to be the most important, even though the value of the feature importance varies across models. Quarterly GDP is a crucial feature for predicting power demand in China. Without quarterly GDP, the evaluating metrics were poor, leading us to conclude that the models for China were unexploitable for generalization. These results highlight the importance of considering economic indicators reflecting the importance of the industrial sector's share in the total power demand, such as quarterly GDP, when developing models for power demand forecasting in China.

415 Overall, Fig. 8 provides insights into the key factors influencing power demand across various countries, highlighting again the crucial role of temperature-related features as a primary driver of power demand. The observed variations in the importance of human activity predictors across different countries and machine-learning regressors suggest the significance of accurately including region-specific characteristics and machine-learning approaches in predicting power demand.

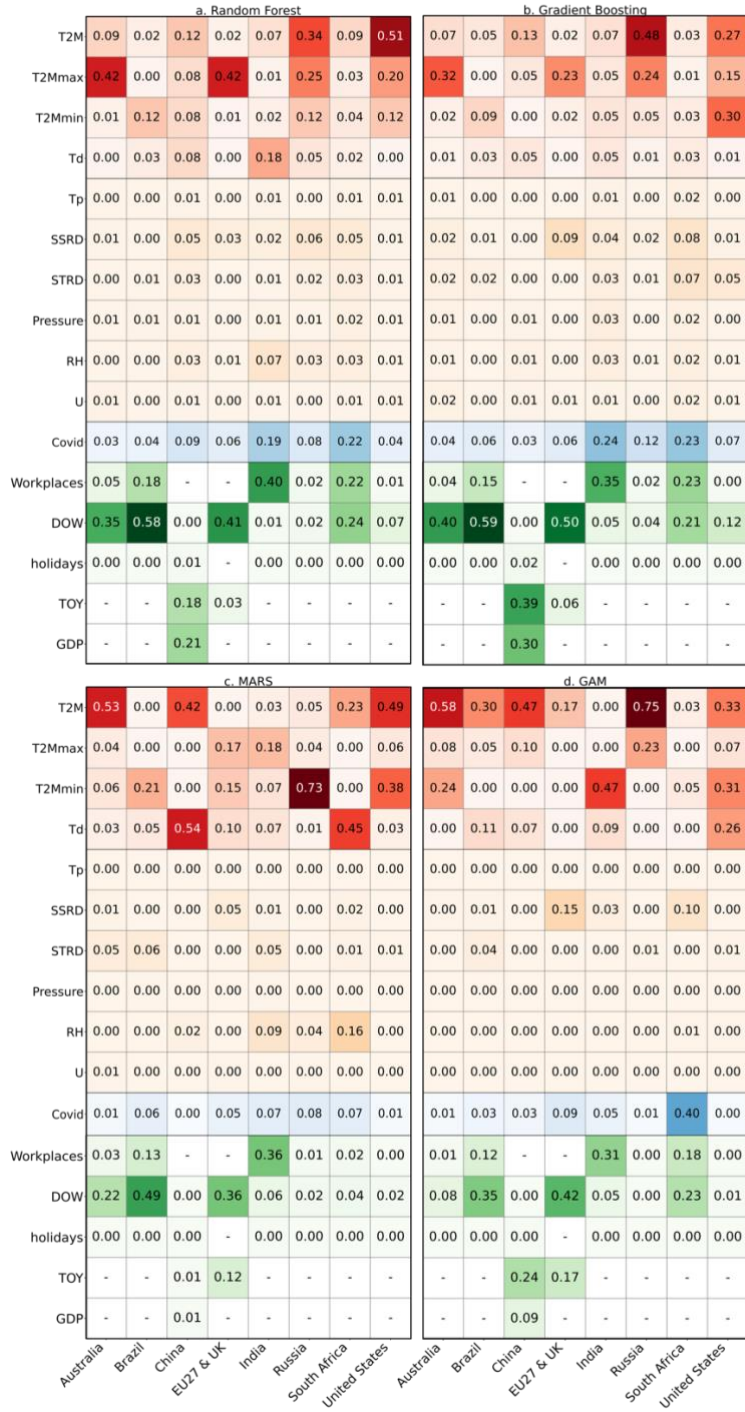
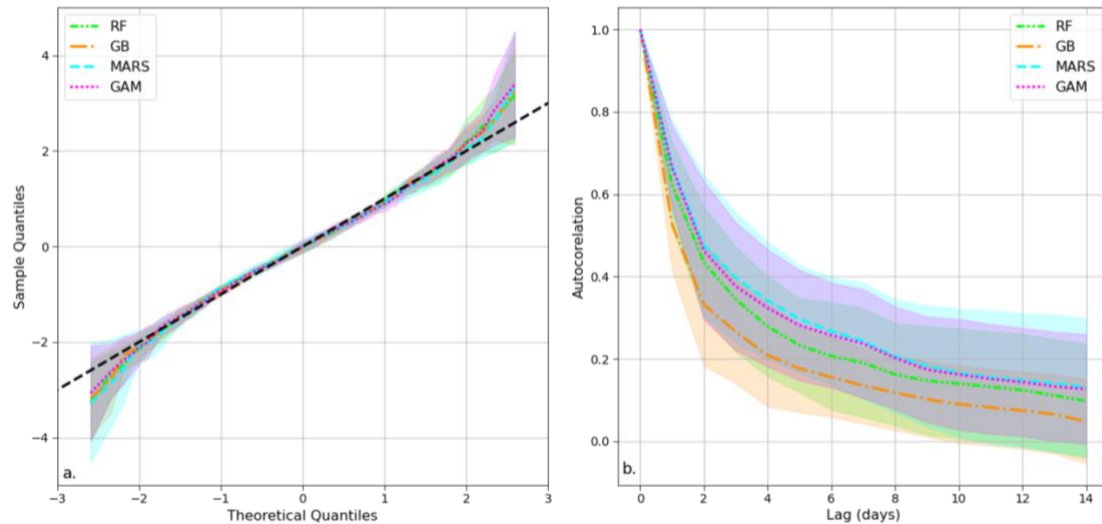


Figure 8. Permutation feature importance for four different machine-learning regressors: (a) RF, (b) GB, (c) MARS, and (d) GAM. The colors represent the different types of predictive features: red for

temperature-related features, orange for other climate-related features, blue for covid, and green for socioeconomic features. The columns correspond to the countries indicated at the bottom of the figure.

425

5.2 Validation and Limits of the Models



430

Figure 9. (a) Quantile-quantile (QQ) plot displaying the mean and standard deviation (shaded area) of the residuals' quantiles for the four models (RF, GB, MARS, and GAM) across eight European countries during the test period. (b) Autocorrelation plot illustrating the average autocorrelation values across the eight countries or regions studied for each of the four models with a 14-day maximum lag. The shaded area represents the standard deviation across countries.

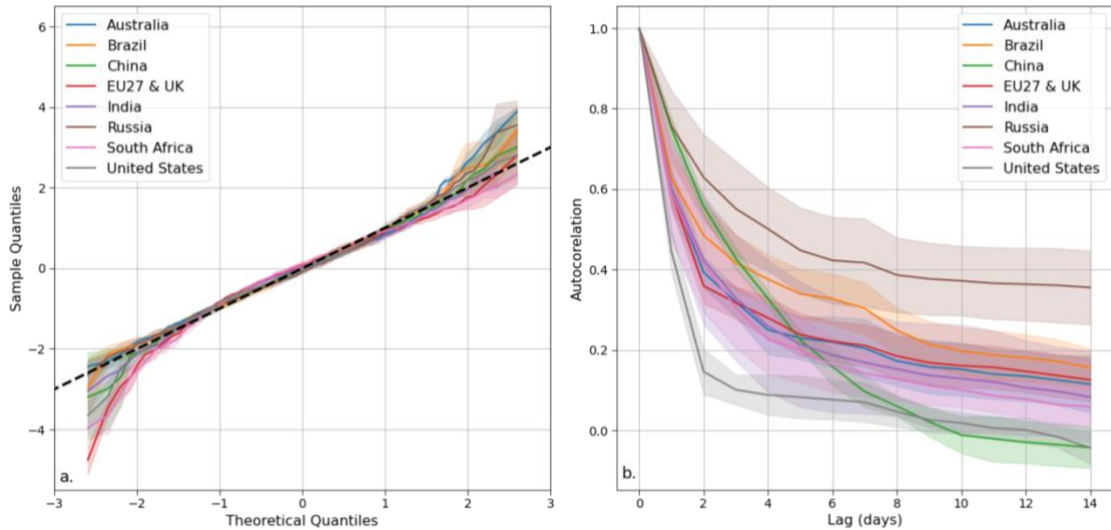


Figure 10. (a) Quantile-quantile (QQ) plot displaying the mean and standard deviation (shaded area) of the residuals' quantiles for all countries across the four models during the test period. (b) Autocorrelation plot illustrating the average autocorrelation values across the four models for all countries with a 14-day maximum lag. The shaded area represents the standard deviation across countries.

The analysis of the residuals of the four models provides information on the performance of the models in predicting the statistical distribution of power demand. We analyzed the performance of the four models using residual quantiles compared to the theoretical Gaussian distribution (Figs. 9a and 10a). This examination is carried out at a global level encompassing all countries and regions (Fig. 9a) and at a country-specific level for each model (Fig. 10a). This analysis reveals that all models perform similarly, with slight deviations from the expected normal distribution within the intermediate quantiles range (between two and minus two) and higher deviations observed above this threshold. Therefore, the Gaussian hypothesis is confirmed, except for extreme values, for which the dataset contains relatively few observations. Those extreme values are often attributed to periods of unusual economic activity, such as bank holidays or specific public holidays that are difficult to model (Srinivasan et al., 1995; Ziel, 2018). Consequently, our models can underestimate or overestimate very low or high power demand, respectively.

The autocorrelation plots of the residuals (Fig. 9b) reveal differences between the models and countries. In particular, gradient boosting outperforms the other models in this respect, with the lowest autocorrelation values. In contrast, MARS shows the highest values. RF and GAM are in between with very similar results. Some countries exhibit superior performances (Fig. 10b). For example, the residual autocorrelation values for Russia

decrease with time at a slower pace than for other countries. Despite the differences in autocorrelation values
455 between the models and across countries, it is worth noting that all models exhibit a similar trend. Specifically, the autocorrelations of the residuals are high up to a lag of a few days, as also reported elsewhere. The autocorrelations drop beyond a lag of a few days, indicating that our models did not miss any significant temporal information.

Overall, these findings are encouraging and validate our models. Therefore, the models can be used for the
460 projection of power demand. However, caution should be exercised when considering extreme values. It is possible to improve the modeling of such values by using a class of quantile regression models. Various types of models have been developed that are specifically designed to address extreme quantiles. One such model is the quantile regression forest, which is a generalization of the random forest model (Meinshausen, 2006). **Recent work by Gnecco et al. (2023) also proposed an approach based on random forest, tailored to extreme quantiles.**

465 Another example is the additive quantile regression model, which has demonstrated promising results in recent studies (Fasiolo et al., 2020). **Finally, Velthoen et al. (2022) developed similar quantile models but for a gradient boosting approach. Such models are consistent with the type of models used in this study and will be applied in future studies to improve the accuracy of power demand projections.**

Overall, while the models developed in this study offer valuable insights into predicting power demand, some
470 limitations must be considered. Firstly, our study period included the COVID-19 pandemic, which significantly impacted energy consumption and emissions (Liu et al., 2020b; García et al., 2021; Aruga et al., 2020). While we incorporate this variable in our models, the extent of its impact may not have been fully captured. Training the regressors on periods not affected by covid might give better results.

Additionally, the irregularity observed in the modeling process for China is worth noting, as China necessitates
475 the inclusion of quarterly GDP to attain good results. Although our approach was largely consistent across countries, it did not achieve a perfect "one-fits-all" approach. Consequently, while this work established a modeling framework applicable to multiple countries, further revisions may be required when extending it to countries not encompassed in this study.

Finally, although all models yielded satisfactory outcomes, each model employed the predictive features in
480 distinct ways (Figs. 4 and 9). Certain predictive features did not exhibit the expected behavior (as shown in Fig. 5b, where T2Mmin showed no sensitivity for lower temperatures). Furthermore, the role and impact of the TOY variable, which functions as a corrective factor for countries where Google Mobility data are not available, remain somewhat ambiguous. While it can account for annually recurring phenomena not elucidated by other predictive features, it would require a more extensive dataset spanning several years to refine its precise function.

485 Addressing these limitations through future research can lead to more accurate and robust models for predicting power demand and related CO₂ emissions.

6 Perspective

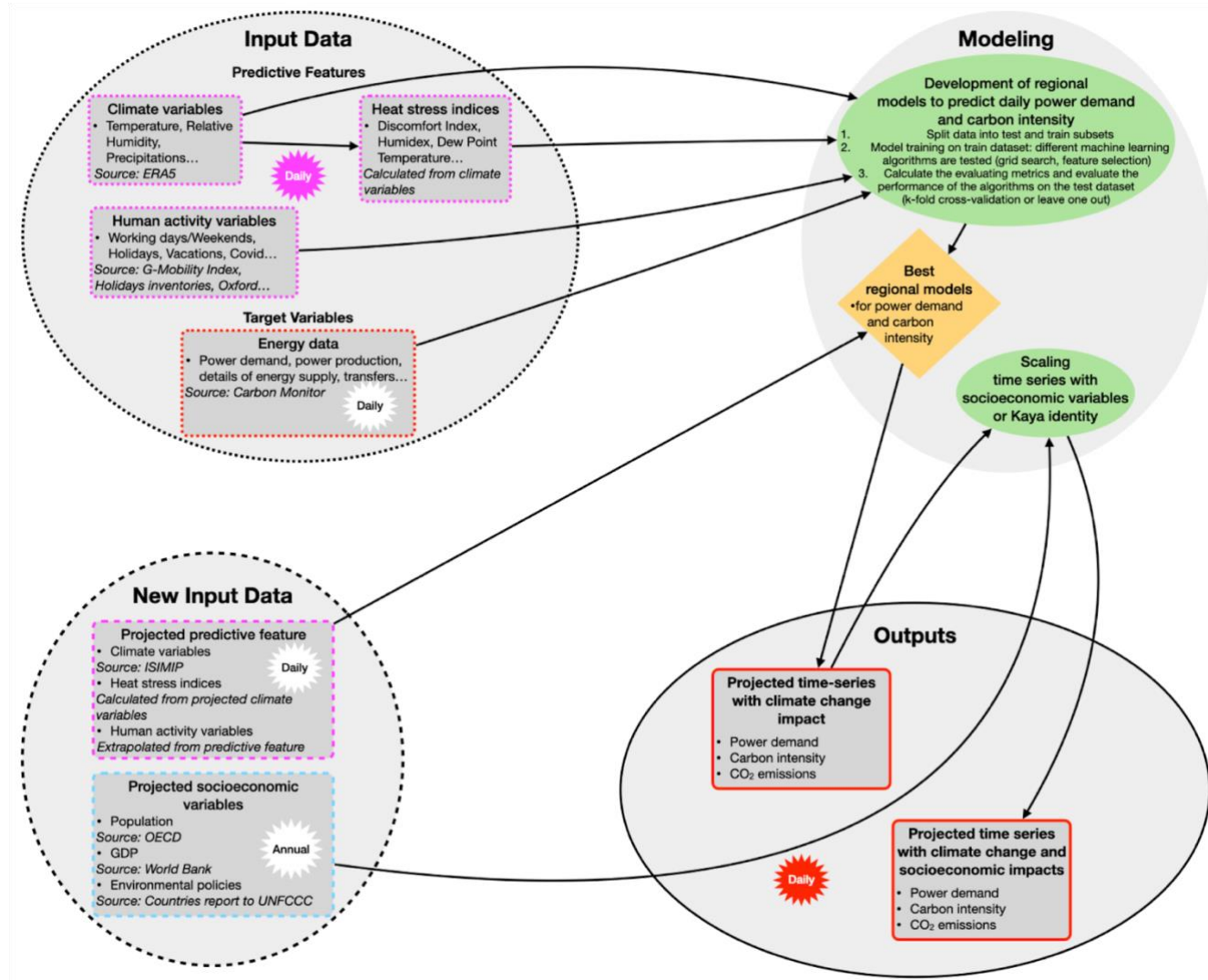


Figure 11. Extended methodological flowchart toward CO₂ emission projections.

490

The present study aims to establish a modeling approach to simulating national daily power demand from climate and human activity features. The proposed approach has the potential to be extended to predict long-term power

495 demand trends under changing climatic conditions and to estimate the corresponding CO₂ emissions resulting from power generation (Fig. 11). This extension would involve developing separate models for simulating power demand and carbon intensity. To achieve this, the target variable would be set as the daily carbon intensity rather than power demand, resulting in the development of two parallel models: one for daily power demand and another for daily carbon intensity. CO₂ emissions are calculated by combining the projections from these two models.

500 To apply this approach, projected climate features obtained from the CMIP6 simulation round, along with projected human activity variables such as DOW (Day of the Week) and Holidays, would be necessary. It should be noted that certain predictive features, such as “workplaces” from the Google Mobility Data, may not be subject to projection. By employing the two abovementioned models, projections of power demand, carbon intensity, and CO₂ emissions can be obtained. Other socioeconomic factors, such as population growth, GDP, and environmental policies, can be incorporated to enhance the projection of daily power demand and CO₂ emissions 505 (Figure 11). By considering the influence of population growth and GDP, the projections of daily power demand can be scaled accordingly. Carbon intensity projections could be developed based on assumed environmental policies aligned with the SSPs (Shared Socioeconomic Pathways) narratives and used to scale the projection of daily carbon intensity obtained with the data-based models. A similar approach has already been applied to Qatar and Japan with different scenarios in alignment with the SSPs narratives (Gurriaran et al., 2022a; Gurriaran et al., 510 2022b).

515 However, our current models lack the ability to account for the future availability of heating and cooling technologies in the different areas under study. To address this significant limitation in projecting long-term trends, our strategy is to apply relationships observed in countries currently equipped with such technologies to countries lacking them. For example, we can simulate European electricity demand by applying the observed electricity-demand-climate relationship in Japan or the US, especially beyond the cooling threshold. By carefully selecting country combinations, we aim to develop future scenarios that are consistent with the narratives of the SSPs.

520 The approach presented in this study has the potential to be extended to evaluate the effectiveness of different policies and initiatives aimed at reducing CO₂ emissions. By considering the influence of changing energy demand under future climate change scenarios, it becomes possible to evaluate the effectiveness of these measures in achieving emission reduction targets. Furthermore, coupling the models developed in this study with simple climate models such as ACC2 (Aggregated Carbon cycle, atmospheric chemistry, and climate model, Tanaka et al., 2007; Tanaka and O'Neill, 2018) enables quantification of the feedback loop between human

activity, CO₂ emissions, climate change, power demand changes, CO₂ emission changes, and the impact on
525 climate (precisely, human activity → CO₂ emissions → climate change → human activity).

In conclusion, the models developed in this study provide a valuable tool for analyzing, forecasting and understanding power demand patterns and CO₂ emissions in the context of climate change across various regions worldwide. Applying these models could offer insights into the potential future scenarios and dynamics of power demand, enabling policymakers and stakeholders to make informed decisions and shape effective energy policies.

530 **Code availability**

Access to the model's source code, stored in a private Zenodo repository, is available upon request at: <https://doi.org/10.5281/zenodo.8135971>. The model is coded in Python (version 3.6.12). The code is not publicly accessible as the primary company associated with the lead author has enforced a strict policy against its public distribution. The company's rationale for this decision is to safeguard its competitive advantage and proprietary
535 algorithms from potential misuse or unauthorized access. The distribution of the code for non-commercial research purposes may be considered upon request to the corresponding author, subject to validation by the primary company. The reviewers were granted access to the code for evaluation purposes.

540 List of Python library necessary:

- Pyearth 0.1.0
- Pandas1.1.5
- Matplotlib3.3.2
- numpy1.19.2
- sklearn0.0
- pygam0.8.0
- PyALE1.1.2
- Statsmodels0.12.2

545 **Data availability**

Climate data used for this study are available from the global atmospheric reanalysis dataset produced by the European Centre for Medium-Range Weather Forecasts (ECMWF) at
550 <https://cds.climate.copernicus.eu/cdsapp#!/home>. Below is the query necessary to download the data with the

CDS toolbox and the list of the climate data names. This query allows you to access the specific variables you need by replacing "VARIABLE_NAME" with the name of the variable you want to download. Energy data are available at <https://power.carbonmonitor.org> (Carbon Monitor – Power). Google Community Mobility Reports data are available at <https://www.google.com/covid19/mobility/>. COVID-19 stringency index data are extracted from the Oxford Coronavirus Government Response Tracker (OxCGRT) project and are available at <https://ourworldindata.org/covid-stringency-index>.

565 ERA5 climate data names: 10m_u_component_of_wind, 10m_v_component_of_wind,
560 2m_dewpoint_temperature, 2m_temperature, relative_humidity, surface_pressure,
surface_solar_radiation_downwards, surface_thermal_radiation_downwards, total_precipitation

```
import cdstoolbox as ct

565 @ct.application(title='Download data')

@ct.output.download()

def download_application():

    data = ct.catalogue.retrieve(
        'reanalysis-era5-land',
        570

        {
            'variable': 'VARIABLE_NAME',
            'year': '2022',
            'month': '01',
            'day': [
                '01', '02', '03', '04', '05', '06', '07', '08', '09', '10', '11', '12',
                '575
                '13', '14', '15', '16', '17', '18', '19', '20', '21', '22', '23', '24',
                '25', '26', '27', '28', '29', '30', '31',
            ]
        }
    )

```

```
    ],
    'time': [
580        '00:00', '01:00', '02:00', '03:00', '04:00', '05:00', '06:00', '07:00', '08:00',
        '09:00', '10:00', '11:00', '12:00', '13:00', '14:00', '15:00', '16:00', '17:00',
        '18:00', '19:00', '20:00', '21:00', '22:00', '23:00',
    ],
    }
585 )
daily_mean = ct.cube.resample(data, freq='day', dim='time', how='mean')

return daily_mean
```

To obtain T2Mmax and T2Mmin, replace `how='mean'`, by `how='max'` and `how='min'`, respectively, in the penultimate line of the query

590 **Supplement**

The supplement related to this article is available online at: <https://doi.org/10.5281/zenodo.8039225>

Author contribution

LG led the design and implementation of the model with inputs from YG and collected the data. LG led the writing of the manuscript, with input from all authors. BZ constituted the Carbon Monitor – Power database. 595 LG, KT, PC, and YG conceptualized the project and participated in the formal analysis of the results. All authors read and approved the manuscript.

Competing interests

The authors declare that they have no conflict of interest.

Acknowledgments

600 KT benefited from State assistance managed by the National Research Agency in France under the Programme d'Investissements d'Avenir under the reference ANR-19-MPGA-0008.

References

ACAPS COVID-19 – Government Measures Dataset: <https://data.humdata.org/dataset/acaps-covid19-government-measures-dataset>, last access: 5 January 2023. 2021

605 Ahmad, A.: Increase in frequency of nuclear power outages due to changing climates, *Nature Energy*, 6, 755, <https://doi.org/10.1038/s41560-021-00849-y>, 2021.

Antoniadis, A., Gaucher, S., and Goude, Y.: Hierarchical transfer learning with applications for electricity load forecasting, *arXiv[preprint]*, *arXiv:2111.08512*, 22 November 2022.

610 Antonopoulos, I., Petropoulos, F., and Hatziargyriou, N.: Artificial intelligence and machine learning approaches to energy demand-side response: a systematic review, *Renewable and Sustainable Energy Reviews*, 130, 109899, <https://doi.org/10.1016/j.rser.2020.109899>, 2020.

Apley, D. W. and Zhu, J.: Visualizing the effects of predictor variables in black box supervised learning models, *Journal of the Royal Statistical Society: Series B (Statistical Methodology)*, 82(4), 1059-1086, <https://doi.org/10.1111/rssb.12377>, 2020.

615 Aruga, K., Monirul Islam, M., and Jannat, A.: Effect of COVID-19 on Indian energy consumption. *Sustainability*, 12(14), 5616, <https://doi.org/10.3390/su12145616>, 2020.

Bloomfield, H.C., Brayshaw, D.J., Shaffrey, L.C., Coker, P.J., and Thornton, H.E.: Quantifying the increasing sensitivity of power systems to climate variability, *Environ. Res. Lett.* 11, 124025, [10.1088/1748-9326/11/12/124025](https://doi.org/10.1088/1748-9326/11/12/124025), 2016.

620 Bloomfield, H.C., Brayshaw, D.J., Charlton-Perez, A.J.: Characterizing the winter meteorological drivers of the European electricity system using targeted circulation types, *Meteorological Applications*, 27(1), e1858.<https://doi.org/10.1002/met.1858>, 2020.

Breiman, L.: Random Forests, *Machine Learning*, 45, 5-32. <http://dx.doi.org/10.1023/A:1010933404324>, 2001.

Burillo, D., Chester, M. V., Pincetl, S., Fournier, E. D., and Reyna, J.: Forecasting Peak Electricity Demand for 625 Los Angeles Considering Higher Air Temperatures due to Climate Change, *Applied Energy*, 236, 1-9, <https://doi.org/10.1016/j.apenergy.2018.11.039>, 2018.

Chambers, J. M.: Graphical Methods for Data Analysis, 1st Edition, Chapman and Hall/CRC, <https://doi.org/10.1201/9781351072304>, 1983.

Chen, T., and Guestrin, C.: XGBoost: A Scalable Tree Boosting System, in: Proceedings of the 22nd ACM SIGKDD, International Conference on Knowledge Discovery and Data Mining, San Francisco, CA, USA, 13-17 August 2016, 785-794, <https://doi.org/10.1145/2939672.2939785>, 2016.

CIEISIN, Center for International Earth Science Information Network - Columbia University, Gridded Population of the World, Version 4 (GPWv4): Population Density, Revision 11, Palisades, New York: NASA Socioeconomic Data and Applications Center (SEDAC), <https://doi.org/10.7927/H49C6VHW>. Accessed 30 May 635 2023. 2018.

Craig, M.T., Cohen, S., Macknick, J., Draxl, C., Guerra, O.J., Sengupta, M. et al.: A review of the potential impacts of climate change on bulk power system planning and operations in the United States. *Renewable and Sustainable Energy Reviews*, 98, 255–267, 2018.

Delort Ylla, J., and Tantet, A., and Drobinski, P., Impacts of Space Heating Electrification on Variable 640 Renewable Energies Regional Mixes and System Total Costs. Available at SSRN: <https://ssrn.com/abstract=4447521> or <http://dx.doi.org/10.2139/ssrn.4447521>, 2023.

Deroubaix, A., Labuhn, I., Camredon, M., Stéfanon, M., and Fantozzi, F.: Large uncertainties in trends of energy demand for heating and cooling under climate change. *Nature Communications*, 12(1), 5197, <https://doi.org/10.1038/s41467-021-25504-8>, 2021.

Dordonnat, V., Pichavant, A., & Pierrot, A.: GEFCom2014 probabilistic electric load forecasting using time 645 series and semi-parametric regression models. *International journal of forecasting*, 32(3), 1005-1011, 2016

Dubus, L., Saint-Drenan, Y.M., Troccoli, A., De Felice, M., Moreau, Y., Ho, L., Goodess, C., Sanger, L.: C3S energy: an operational service to deliver power demand and supply for different electricity sources, time and spatial scales over Europe, <https://doi.org/10.31223/X5MM06>, 2021.

Fan, S. and Hyndman, R. J.: Forecasting electricity demand in Australian National Electricity Market, IEEE 650 Power and Energy Society General Meeting, San Diego, CA, USA, 2012, pp. 1-4, doi: 10.1109/PESGM.2012.6345304, 2012.

Elliston, B., MacGill, I. & Diesendorf, M.: Least cost 100% renewable electricity scenarios in the Australian National Electricity Market. *Energy Policy*, 59, 270–282, 2013

Fasiolo, M., Wood, S. N., Zaffran, M., Nedellec, R., and Goude, Y.: Fast calibrated additive quantile regression, Journal of the American Statistical Association, 116:535, 1402-1412, 10.1080/01621459.2020.1725521, 2020.

Fisher, W. D: On Grouping for Maximum Homogeneity, *Journal of the American Statistical Association*, 53, 789-798, 1958.

660 Flom, P. L., and Cassell, D. L.: Stopping stepwise: Why stepwise and similar selection methods are bad, and what you should use, *NorthEast SAS Users Group*, 2007.

Friedman, J.: Multivariate Adaptive Regression Splines, *Ann. Statist.*, 19(1), 1-67, <https://doi.org/10.1214/aos/1176347963>, 1991.

665 García, S., Parejo, A., Personal, E., Ignacio Guerrero, J., Biscarri, F., and León, C.: A retrospective analysis of the impact of the COVID-19 restrictions on energy consumption at a disaggregated level, *Applied Energy*, 287, 116547, <https://doi.org/10.1016/j.apenergy.2021.116547>, 2021.

Google LLC, Google Mobility Reports, Data file. Retrieved from <https://www.google.com/covid19/mobility/>, 2020.

670 Gurriaran, L., Tanaka, K., Bayram, I. S., Proestos, Y., Lelieveld, J., and Ciais, P.: Warming-induced increase in power demand and CO₂ emissions in Qatar and the Middle East, *Journal of Cleaner Production*, 382, 135359, <https://doi.org/10.1016/j.jclepro.2022.135359>, 2022a.

Gurriaran, L., Tanaka, K., Kiyoshi, T., and Ciais, P.: How climate change may shift power demand in Japan: Insights from data-driven analysis, *ESS Open Archive*, 10.22541/essoar.167214562.25201708/v1, 27 December 2022, 2022b.

675 Hale, T., Angrist, N., Goldszmidt, R., et Kira, B., Petherick, A., Phillips, T., Webster, S., Cameron-Blake, E., Hallas, H., Saptarshi Majumdar, S., and Tatlow, H.: A global panel database of pandemic policies (Oxford COVID-19 Government Response Tracker). *Nature Human Behaviour*, 5, 529–538. <https://doi.org/10.1038/s41562-021-01079-8>, 2021.

Harrell, F. E.: Regression modeling strategies: With applications to linear models, logistic regression, and survival analysis, Second Edition, Springer-Verlag, ISBN: 978-3-319-19425-7, 2001.

680 Hastie, T. J., and Tibshirani, R. J.: Generalized Additive Models, Second Edition, Chapman & Hall/CRC. ISBN 978-0-412-34390-2, 1990.

Hiruta, Y., Gao, L., and Ashina, S.: A novel method for acquiring rigorous temperature response functions for electricity demand at a regional scale, *Science of the Total Environment*, 819, 152893, <https://doi.org/10.1016/j.scitotenv.2021.152893>, 2022a.

685 Hiruta, Y., Ishizaki, N. N., Ashina, S., and Takahashi, K.: Regional and temporal variations in the impacts of future climate change on Japanese electricity demand: Simultaneous interactions among multiple factors

considered, Energy Conversion and Management: X, 14, 100172, <https://doi.org/10.1016/j.ecmx.2021.100172>, 2022b.

690 Hong, T., Pinson, P., Fan, S., Zareipour, H., Troccoli, A., Hyndman, R.J.: Probabilistic energy forecasting: Global Energy Forecasting Competition 2014 and beyond, International Journal of Forecasting, 32, 3, 896-913, <https://doi.org/10.1016/j.ijforecast.2016.02.001>, 2016.

Hyndman, R. J., and Athanasopoulos, G.: Forecasting: principles and practice, 2nd edition, OTexts: Melbourne, Australia. OTexts.com/fpp2, 2018.

695 IEA (International Energy Agency), Global Energy Review 2021. Retrieved from <https://www.iea.org/reports/global-energy-review-2021>, 2021.

Isaac, M., and van Vuuren, D. P.: Modeling global residential sector energy demand for heating and air conditioning in the context of climate change, Energy Policy, 37(2), 507-521, <https://doi.org/10.1016/j.enpol.2008.09.051>, 2009.

700 Jiang, P., Khishgee, S., Alimujiang, A., and Dong, H.: Cost-effective approaches for reducing carbon and air pollution emissions in the power industry in China. Journal of Environmental Management, 264, 110452. <https://doi.org/10.1016/j.jenvman.2020.110452>, 2020.

Ke, G., Meng, Q., Finley, T., Wang, T., Chen, W., Ma, W., Ye, Q., and Liu, T-Y.: LightGBM: A Highly Efficient Gradient Boosting Decision Tree, in: Advances in Neural Information Processing Systems 30, ISBN: 9781510860964, 2017.

705 Liu, Z., Ciais, P., Deng, Z., Lei, R., Davis, S. J., Zheng, B., Wang, Y., Cui, D., Zhu, B., Dou, X., Ke, P., Sun, T., Guo, R., Zhong, H., Boucher, O., Bréon, F-M., Lu, C., Guo, R., Xue, J., Boucher, E., Tanaka, K., and Chevallier, F.: Carbon Monitor, a near-real-time daily dataset of global CO₂ emission from fossil fuel and cement production, Scientific data, 7(1), 392. <https://doi.org/10.1038/s41597-020-00708-7>, 2020a.

710 Liu, Z., Ciais, Deng, Z., Lei, R., Davis, S. J., Feng, S., Zheng, B., Cui, D., Dou, X., Zhu, B., Guo, R., Ke, P., Sun, T., Lu, C., He, P., Wang, Y., Yue, X., Wang, Y., Lei, Y., Zhou, H., Cai, Z., Wu, Y., Guo, R., Han, T., Xue, J., Boucher, O., Boucher, E., Chevallier, F., Tanaka, K., Wei, Y., Zhong, H., Kang, C., Zhang, N., Chen, B., Xi, F., Liu, M., Bréon, F-M., Lu, Y., Zhang, Q., Guan, D., Gong, P., Kammen, D.M., He, K., and Schellnhuber, H. J.: Near-real-time monitoring of global CO₂ emissions reveals the effects of the COVID-19 pandemic. Nature Communications, 11(1), 5172. <https://doi.org/10.1038/s41467-020-18922-7> 2022b.

715 Lucon, O., Ürge-Vorsatz, D., Zain Ahmed, A., Akbari, H., Bertoldi, P., Cabeza, L. F., ... and Vandeveer, S. D. Buildings. In O. Edenhofer, R. et al. (Eds.), Climate Change 2014: Mitigation of Climate Change. Contribution of

Working Group III to the Fifth Assessment Report of the Intergovernmental Panel on Climate Change (pp. 1-68), Cambridge University Press, 2014.

Mathieu, E., Ritchie, H., Rodés-Guirao, L., Appel, C., Giattino, C., Hasell, J., Macdonald, B., Dattani, S.,
720 Beltekian, D., Ortiz-Ospina, E., and Roser, M.: Coronavirus pandemic (COVID-19). Our World in Data. Retrieved from <https://ourworldindata.org/coronavirus>, 2020.

Meinshausen, N.: Quantile regression forests, *Journal of Machine Learning Research*, 7, 983-999, 2006.

Mohammadiziazi, R., and Bilec, M.: Application of machine learning for predicting building energy use at different temporal and spatial resolution under climate change in USA, *Buildings*, 10(8), 139,
725 https://doi.org/10.3390/buildings10080139, 2020.

Mukherjee, S., Vineeth, C. R., and, Nateghi, R.: Evaluating regional climate-electricity demand nexus: A composite Bayesian predictive framework, *Applied Energy*, 235, 1561-1582.
https://doi.org/10.1016/j.apenergy.2018.11.064, 2019.

Muñoz Sabater, J.: ERA5-Land hourly data from 1981 to present. Copernicus Climate Change Service (C3S)
730 Climate Data Store (CDS). <https://doi.org/10.24381/cds.e2161bac>, 2019.

Nedellec, R., Cugliari, J., & Goude, Y.: GEFCom2012: Electric load forecasting and backcasting with semi-parametric models. *International Journal of forecasting*, 30(2), 375-381, 2014

Obst, D., De Vilmarest, J., & Goude, Y.: Adaptive methods for short-term electricity load forecasting during COVID-19 lockdown in France. *IEEE transactions on power systems*, 36(5), 4754-4763, 2021.

735 Pierrot, A., & Goude, Y.: Short-term electricity load forecasting with generalized additive models. *Proceedings of ISAP power*, 2011.

Raschka, S.: Model Evaluation, Model Selection, and Algorithm Selection in Machine Learning. arXiv[preprint], arXiv:1811.12808, 11 November 2020.

Raschka, S., and and Mirjalili, V.: Python Machine Learning, Third Edition, Packt Publishing. ISBN
740 9781789955750, 2019.

Romitti, Y. and Sue Wing, I., Heterogeneous climate change impacts on electricity demand in world cities circa mid-century, *Scientific Reports*, 12, 4280, <https://doi.org/10.1038/s41598-022-07922-w>, 2022.

745 Silva, V. et al. Anticipating Some of the Challenges and Solutions for 60% Renewable Energy Sources in the European Electricity System. In: Drobinski, P., Mougeot, M., Picard, D., Plougonven, R., Tankov, P. (eds) *Renewable Energy: Forecasting and Risk Management. FRM 2017. Springer Proceedings in Mathematics & Statistics*, vol 254. Springer, Cham. https://doi.org/10.1007/978-3-319-99052-1_9, 2018.

Srinivasan, D., Chang, C. S., and Liew. A. C.: Demand forecasting using fuzzy neural computation, with special emphasis on weekend and public holiday forecasting, *IEEE Transactions on Power Systems*, 10(4), 1897-1903, 10.1109/59.476055, 1995.

750 Steadman, R. G.: The assessment of sultriness. Part I: A temperature-humidity index based on human physiology and clothing science, *Journal of Applied Meteorology*, 18, 861-873, [https://doi.org/10.1175/1520-0450\(1979\)018<0861:TAOSPI>2.0.CO;2](https://doi.org/10.1175/1520-0450(1979)018<0861:TAOSPI>2.0.CO;2), 1979.

Tanaka, K., Kriegler, E., Bruckner, T., Hooss, G., Knorr, W., and Raddatz, T.: Aggregated Carbon Cycle, Atmospheric Chemistry, and Climate Model (ACC2) – description of the forward and inverse modes, *Reports on Earth System Science*, 40, Max Planck Institute for Meteorology, Hamburg, 2007.

755 Tanaka, K., and O'Neill, B.: The Paris Agreement zero-emissions goal is not always consistent with the 1.5 and 2°C temperature targets, *Nature Climate Change*, 8, 319–324, <https://doi.org/10.1038/s41558-018-0097-x>, 2018.

Tantet A, Stéfanon M, Drobinski P, Badosa J, Concettini S, Cretì A, D'Ambrosio C, Thomopoulos D, Tankov P.e4clim 1.0: The Energy for a Climate Integrated Model: Description and Application to Italy. *Energies*, 760 12(22):4299. <https://doi.org/10.3390/en12224299>, 2019.

Taylor, K. E.: Summarizing multiple aspects of model performance in a single diagram, *Journal of Geophysical Research*, 106(D7), 7183-7192, <https://doi.org/10.1029/2000JD900719>, 2001.

Toktarova, A., Gruber, L., Hlusiak, M., Bogdanov, D., Breyer, C.: Long term load projection in high resolution for all countries globally, *International Journal of Electrical Power & Energy Systems*, 111, 160-181, 765 <https://doi.org/10.1016/j.ijepes.2019.03.055>, 2019.

Van Ruijven, B., De Cian, E., and Wing, I. S.: Amplification of future energy demand growth due to climate change, *Nature Communications*, 10, 2762, <https://doi.org/10.1038/s41467-019-10399-3>, 2019.

Wood, S. N.: Generalized Additive Models: An Introduction with R, Second Edition, Chapman and Hall/CRC. <https://doi.org/10.1201/9781315370279>, 2017.

770 Yalew, S. G., van Vliet, M. T. H., Gernaat, D. E. H. J., Ludwig, F., Miara, A. Park, C., Byers, E., De Cian, E., Piontek, F., Iyer, G., Mouratiadou, I., Glynn, J., Hejazi, M., Dessens, O., Rochedo, P., Pietzcker, R., Schaeffer, R., Fujimori, S., Dasgupta, S., Mima, S., Santos da Silva, S.R., Chaturvedi, V., Vautard, R., and P. van Vuuren D.P.: Impacts of climate change on energy systems in global and regional scenarios, *Nature Energy*, 5, 794–802, <https://doi.org/10.1038/s41560-020-0664-z>, 2020.

775 Zhu, B., Song, X., Deng, Z., Zhao, W., Huo, D., Sun, T., Ke, P., Cui, D., Lu, C., Zhong, H., Hong, C., Qiu, J., Davis, S. J., Gentine, P., Ciais, P., and Liu, Z.: Carbon Monitor-Power: near-real-time monitoring of global

power generation on hourly to daily scales, *Scientific Data* 10, 217, <https://doi.org/10.1038/s41597-023-02094-2>, 2023.

Ziel, F.: Modeling public holidays in load forecasting: a German case study, *Journal of Modern Power Systems*

780 and Clean Energy

6(2), 191-207, 10.1007/s40565-018-0385-5, 2018.